AGU PUBLICATIONS

JGR

Journal of Geophysical Research: Atmospheres

RESEARCH ARTICLE
10.1002/2014JD022976

Key Points:
- The application of IR cloud clearing for radiance assimilation in NWP
- The benefits of assimilating AIRS/MODIS cloud-cleared radiances are discussed
- Forecasts are substantially improved with assimilating cloud-cleared radiances

Correspondence to:
P. Wang,
pei.wang@ssec.wisc.edu

Citation:
Wang, P., J. Li, M. D. Goldberg, T. J. Schmit, A. H. N. Lim, Z. Li, H. Han, J. Li, and S. A. Ackerman (2015), Assimilation of thermodynamic information from advanced infrared sounders under partially cloudy skies for regional NWP, *J. Geophys. Res. Atmos.*, *120*, doi:10.1002/2014JD022976.

Received 10 DEC 2014
Accepted 12 MAY 2015
Accepted article online 15 MAY 2015

Assimilation of thermodynamic information from advanced infrared sounders under partially cloudy skies for regional NWP

Pei Wang[1,2], Jun Li[1], Mitchell D. Goldberg[3], Timothy J. Schmit[4], Agnes H. N. Lim[1], Zhenglong Li[1], Hyojin Han[1], Jinlong Li[1], and Steve A. Ackerman[1]

[1]Cooperative Institute for Meteorological Satellite Studies, University of Wisconsin-Madison, Madison, Wisconsin, USA, [2]Department of Atmospheric Science and Oceanic Sciences, University of Wisconsin-Madison, Madison, Wisconsin, USA, [3]NOAA JPSS Program Office, Lanham, Maryland, USA, [4]Center for Satellite Applications and Research, NOAA/NESDIS, Madison, Wisconsin, USA

Abstract Generally, only clear-infrared spectral radiances (not affected by clouds) are assimilated in weather analysis systems. This is due to difficulties in modeling cloudy radiances as well as in observing their vertical structure from space. To take full advantage of the thermodynamic information in advanced infrared (IR) sounder observations requires assimilating radiances from cloud-contaminated regions. An optimal imager/sounder cloud-clearing technique has been developed by the Cooperative Institute for Meteorological Satellite Studies at the University of Wisconsin-Madison. This technique can be used to retrieve clear column radiances through combining collocated multiband imager IR clear radiances and the sounder cloudy radiances; no background information is needed in this method. The imager/sounder cloud-clearing technique is similar to that of the microwave/IR cloud clearing in the derivation of the clear-sky equivalent radiances. However, it retains the original IR sounder resolution, which is critical for regional numerical weather prediction applications. In this study, we have investigated the assimilation of cloud-cleared IR sounder radiances using Atmospheric Infrared Sounder (AIRS)/Moderate Resolution Imaging Spectroradiometer for three hurricanes, Sandy (2012), Irene (2011), and Ike (2008). Results show that assimilating additional cloud-cleared AIRS radiances reduces the 48 and 72 h temperature forecast root-mean-square error by 0.1–0.3 K between 300 and 850 hPa. Substantial improvement in reducing track forecasts errors in the range of 10 km to 50 km was achieved.

1. Introduction

The advantages of high spectral resolution infrared (IR) measurements to numerical weather prediction (NWP) are improved vertical temperature and moisture resolution, better definition of cloud properties, and more accurate surface emissivity estimates. Using the global model at the National Center for Environmental Prediction (NCEP), *Le Marshall et al.* [2006] had showed significant positive impact on the 500 hPa height anomaly correlation over both the Northern and Southern Hemispheres, with high spectral resolution AIRS (Atmospheric Infrared Sounder) data compared to the coarse spectral resolution of the High-resolution Infrared Radiation Sounder (HIRS), a 20-channel IR sounder flown on the NOAA Polar Orbiting Environmental Satellites series. Many NWP centers have reported similar positive impacts from the assimilation of AIRS radiances under clear sky, including NCEP [*Le Marshall et al.*, 2005a, 2005b, 2006], the European Center for Medium-Range Weather Forecasts [*McNally et al.*, 2006], the Meteo-France [*Auligné et al.*, 2003], the UK Meteorological Office [*Cameron et al.*, 2005], and Japan Meteorological Agency [*Okamoto et al.*, 2008]. In addition, after taking into account the greater number of Advanced Microwave Sounder Unit (AMSU) sensors assimilated, the impact of AIRS radiance assimilation is on the same scale as that from the AMSU data [*Cardinali*, 2009].

A large percentage of observations from IR sounders are affected by clouds. The chance of a field of view (FOV) being affected by clouds is approximately 75% for HIRS [*Wylie et al.*, 1994] and around 87% for AIRS [*Rienecker et al.*, 2008]. This means that a majority of IR sounder radiance observations are abandoned for assimilation if only clear-sky IR radiances are used. To expand advanced IR sounder radiance assimilation in cloudy regions, research has been conducted on assimilating the cloudy radiances directly [*Heilliette and Garand*, 2007; *Pavelin et al.*, 2008]. *Stengel et al.* [2013] assimilated the Spinning Enhanced Visible and

Infrared Imager cloud-affected IR radiances with a four-dimensional incremental variational assimilation (4D-Var) system and reduced forecast fields normalized error between 500 hPa and 200 hPa by 4%, the forecast error of geopotential height and humidity by 1%, and forecast error of wind direction by 1–3% in the upper troposphere. However, some negative impacts were noted in the lower troposphere. To date, cloudy radiances have not been effectively used operationally due to various factors: modeling clouds in NWP, calculating equivalent radiances from radiative transfer models, and observing the vertical structures of cloud parameters (fraction, liquid water content, and phase) [*Errico et al*., 2007; *Geer and Bauer*, 2011].

Studies [*Pangaud et al*., 2009; *Wang et al*., 2014] found that if the cloudy radiances are assimilated as clear observations, there will be a negative impact on the quality of the NWP analysis. Therefore, reliable cloud detection is essential. The first step is to reject all FOVs containing clouds and only keep completely clear FOVs (referred to as clear pixel detection) [*English et al*., 1999]. With the cloud mask from the collocated MODIS (Moderate Resolution Imaging Spectroradiometer) [*Nagle and Holz*, 2009], AIRS subpixel cloud detection and characterization can be derived [*Li et al*., 2004]. Using a strict cloud mask algorithm, this technique ensures high-quality clear radiances will be assimilated. A limitation, however, is a reduction in the number of observations. *McNally and Watts* [2003] demonstrated that assimilating cloud insensitive radiance observations (referred to as clear channel detection) shows positive impact on the analysis and forecast. However, any cloud contamination would degrade the analysis fields. *Wang et al*. [2014] compared these two cloud detection methods (clear pixel detection and clear channel detection) for Hurricane Sandy (2012) forecasts. It was found that the clear channel method may fail to reject some cloudy radiance and assimilated them as clear ones, which introduces a cold bias in the temperature field and a wet bias in the moisture field.

The availability of observations that can be effectively assimilated is limited if only clear IR radiances are used. To enable assimilating thermodynamic information in partially cloudy regions, cloud-cleared radiances are assimilated into a regional NWP model in this study. The motivations for assimilating cloud-cleared advanced IR sounder radiances are the following:

1. Currently, most operational NWP centers use clear radiances (either clear field of view radiances or radiances from channels not affected by clouds). Expanding radiance assimilation into partially cloudy regions is needed to maximize the utility of advanced IR sounder data
2. Research using cloudy radiances directly has been ongoing, but significant challenges remain. For example, both NWP and radiative transfer models have relatively large uncertainties in simulating cloudy situations. There is a temperature sensitivity (Jacobian) jump at the cloud level, which is another factor making assimilation difficult. In addition, there might be inconsistencies between NWP estimated clouds and the satellite. For example, the NWP background field may be clear while the satellite observation indicates clouds, or vice versa.

In this study, we use AIRS cloud-cleared radiances since the AIRS clear radiances have been successfully used in operational NWP forecasts. We have compared stand-alone AIRS cloud-cleared radiances with those benefiting from collocation with MODIS—so called AIRS/MODIS cloud clearing [*Li et al*., 2005]. This method retrieves clear column radiances through combining collocated multiband MODIS IR clear radiances and the AIRS cloudy radiances [*Li et al*., 2004]. No NWP background information is needed in the AIRS/MODIS cloud-clearing technique. MODIS is used to cloud clear the AIRS radiances as well as to quality control the cloud-cleared radiances [*Goldberg et al*., 2005]. Approximately 13% of the AIRS FOVs are under clear skies, and an additional 21% of the AIRS FOVs can be cloud cleared successfully [*Rienecker et al*., 2008]. Global NWP assimilation experiments using the Goddard Earth Observing System Model, Version 5 (GEOS-5) at NASA Global Modeling and Assimilation Office (GMAO) indicated that the forecast skill in the troposphere was improved through assimilation of the cloud-cleared AIRS radiances as they provide useful sounding information beneath the clouds. However, the coarse horizontal resolution ($1° \times 1.25°$) of GEOS-5 is not ideal for mesoscale applications, especially for hurricane forecasts.

The AIRS/MODIS cloud-cleared radiances are tested with a Cooperative Institute for Meteorological Satellite Studies (CIMSS) research test bed called SDAT (Satellite Data Assimilation for Tropical storm forecasts: http://cimss.ssec.wisc.edu/sdat), SDAT combines the community Grid point Statistical Interpolation (GSI) assimilation system and the advanced Weather Research Forecast (WRF) model [*Li et al*., 2014]. It consists of data preparation, assimilation, and forecast steps. Using the SDAT framework, there is substantial

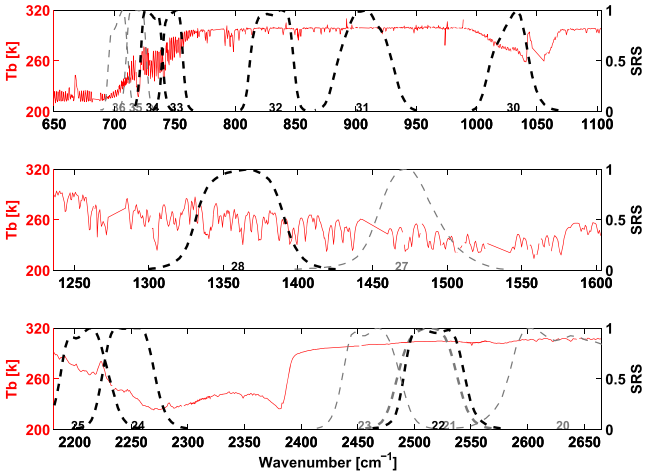

Figure 1. AIRS brightness temperature (BT) spectrum (red, unit: K) with MODIS spectral response functions of selected channels (dashed). MODIS channel numbers are marked in the figure. Black is MODIS channels used in cloud clearing and QC, grey is not used.

improvement on Tropical Cyclone (TC) track forecasts when cloud-cleared IR sounder radiances are included in the assimilation compared with forecasts that assimilate clear radiances only.

Section 2 briefly introduces the methodology of AIRS/MODIS cloud clearing. Section 3 describes the data assimilation system and the NWP model, as well as the experimental design. Sections 4 and 5 discuss the influences on analysis fields and forecasts, respectively. The conclusions are summarized in section 6.

2. Methodology

Smith et al. [2004] had discussed several possible methods of extracting atmospheric thermodynamic information from cloud-contaminated hyperspectral infrared measurements: (1) cloud-clearing method based upon the spatially adjacent cloud-contaminated radiances, (2) retrieval method using the assumption of opaque and overcast cloudy conditions, where only sounding down to the cloud level is possible, and (3) retrieval or assimilation method using an accurate cloud radiative transfer model, which physically accounts for absorption and scattering of cloud particles within the field of view (FOV) of the measurements. Unlike the other two methods, the first approach handles clouds indirectly by using multiple spatial FOVs to extract the clear portion of the observations. In other words, cloud-clearing extracts the radiance arising from the clear air portion of the partly cloudy FOVs by extrapolating spatially coherent cloudy radiances. Thus, the cloud-cleared radiances can be assimilated as in the clear field of view case.

Using the collocated clear portion of MODIS IR radiances within the two adjacent AIRS FOVs' cloudy radiances, a cloud-clearing parameter call N* can be derived by spatially averaging MODIS clear radiances to AIRS footprints and spectrally convolving AIRS radiances to MODIS bands by applying MODIS Spectral Response Functions (SRFs) to the AIRS radiance spectrum (see Figure 1 for the MODIS SRFs overlaying on an AIRS brightness temperature spectrum). Once N* is derived, it can be applied to the cloudy radiances from these two FOV's measurements and derive the clear equivalent radiance spectrum representing the common clear portion of radiances within the two adjacent AIRS FOVs. This N* concept for AIRS/MODIS cloud clearing was described by *Smith et al.* [2004] with a single MODIS band (11 μm) and was further expanded to use multiple MODIS spectral bands [*Li et al.*, 2005] through optimal cloud clearing.

Once the cloud-cleared AIRS radiance spectrum is produced, a two-step evaluation of quality control (QC) is applied to ensure the quality of the cloud-cleared radiances [*Li et al.*, 2005]. In the first step, AIRS cloud-cleared radiances are convolved with a MODIS spectral response function to form pseudo-MODIS radiances. They are compared with spatially averaged MODIS clear radiances within the FOV in consideration [*Goldberg et al.*, 2005]. Those with large differences are thrown away. A threshold of 0.3 K is set for quality control on the differences between the simulated AIRS cloud-cleared (convolved to MODIS IR bands) radiances and the MODIS IR band clear radiance observations in this study. In the second step, the cloud-cleared radiances are compared with immediate clear neighbor FOVs to ensure reasonable spatial variations. These differences must all be smaller than the predetermined expected error. Otherwise, the whole cloud-cleared AIRS spectra are rejected for assimilation. Nine MODIS infrared bands (22 (3.959 μm), 24 (4.465 μm), 25 (4.515 μm), 28 (7.325 μm), 30 (9.73 μm), 31 (11.03 μm), 32 (12.02 μm), 33 (13.335 μm), and 34 (13.635 μm)) are used in both the cloud clearing and QC process. MODIS bands 20 (3.750 μm), 23 (4.050 μm), and 27 (6.715 μm) are not used in both cloud clearing and QC because of the convolution error introduced by the spectral gaps in the AIRS spectrum. Band 21 has not been included due to the large detector noise. Bands 35 (13.935 μm) and 36 (14.235 μm) are not used due to the

calibration error of the spectral response function. Therefore, the AIRS cloud-cleared radiances have high quality and can be treated as equivalent clear radiances for assimilation. The technique for assimilating clear-sky radiances can be applied directly to the cloud-cleared radiances without modification of GSI system.

3. Experimental Design and NWP Model

3.1. Hurricanes

Hurricanes Sandy (2012), Irene (2011), and Ike (2008) over the Atlantic Ocean are the selected case studies for the assimilation and forecast experiments. Sandy was a very destructive hurricane during the 2012 Atlantic hurricane season. It was a late-season hurricane that developed on 1200 UTC 22 October in the southwestern Caribbean Sea, and then moved northward. By 25 October when Sandy made landfall in Cuba, it was a Category 3 storm. After passing the Bahamas, Sandy turned toward the northeast around 1200 UTC 27 October, and its speed increased again by 1200 UTC 27 October. On 28 October, Sandy passed southeast of North Carolina and turned to the northwest. By 2100 UTC 29 October, Sandy became an extratropical storm and the center of posttropical Cyclone Sandy made landfall at about 2300 UTC near Brigantine, New Jersey [*Blake et al*., 2013]. Throughout its path across seven countries, Sandy caused widespread destruction with estimated damage over $68 billion (U.S. dollars), and the total fatalities were at least 286. The total losses of Hurricane Sandy put it second only to Hurricane Katrina (2005).

Hurricane Irene (2011) formed east of the Lesser Antilles on 0000 UTC 21 August 2011. By 1200 UTC 24 August, it had increased in strength to become a major hurricane (Category 3) and turned northward. It passed offshore the east coast of Florida and Georgia around 1200 UTC 25 August. Irene made landfall near Cape Lookout, North Carolina at 1200 UTC 27 August. Irene continued to move north and northeastward and made landfall again near Atlantic City, New Jersey, at 0935 UTC on 28 August 2011 [*Avila and Cangialosi*, 2011]. Irene killed at least 56 people and caused an estimated $15.6 billion in total damage in the United States.

Hurricane Ike (2008) was a destructive tropical cyclone that became a hurricane by 1800 UTC 3 September 2008, and a Category 4 storm at 0600 UTC 4 September. It moved from North Atlantic Ocean westward and made landfall in Cuba around 0200 UTC 8 September. Ike continued moving westward across Cuba and then turned northwest to make final landfall in Texas on 0700 UTC 13 September [*Berg*, 2009]. Ike was directly responsible for at least 103 deaths throughout its path. The damages from Ike in U. S. are estimated at $29.5 billion with additional $7.3 billion in Cuba.

3.2. Assimilation System

The GSI system version 3.1 from the Developmental Test bed Center (DTC) is used as the data assimilation model. GSI is primarily a three-dimensional incremental variational system with modules developed for advanced features for both global and regional applications [*Wu et al*., 2002; *Kleist et al*., 2009]. For the GSI user guide, see http://www.dtcenter.org/comGSI/users/docs/users_guide/ GSIUserGuide_v3.1.pdf. GSI is an operational assimilation system developed jointly by NOAA, NASA, and National Center for Atmospheric Research (NCAR). DTC transitioned the operational GSI system into a community system to be used in the public domain for case studies or research. It is capable of assimilating various kinds of observations from conventional data to aerosol observations and satellite radiance data. The GSI system is now widely used in the research community [*Schwartz et al*., 2012; *Zhang et al*., 2013; *Lim et al*., 2014].

The Community Radiative Transfer Model (CRTM) developed by the Joint Center for Satellite Data Assimilation has been implemented into the GSI system as its fast radiative transfer model [*Han et al*., 2006; *Weng*, 2007; *Chen et al*., 2010, 2012]. CRTM simulates the radiances and radiance Jacobians at the top of the atmosphere. The CRTM coefficients version 2.0.5 is used in the GSI.

3.3. Forecast Model

The advanced research version of the Weather Research and Forecasting (WRF-ARW) model version 3.2.1 is used as the NWP system. WRF is a mesoscale NWP model, which is designed for both research and operational forecasting. The NCAR Mesoscale and Microscale Meteorology Division support WRF-ARW for the community. The equation set for WRF-ARW is fully compressible, Eulerian, and nonhydrostatic with a run-time hydrostatic option [*Skamarock et al*., 2008]. In WRF-ARW, several physical schemes are available

Table 1. Data Used in the Experiments (Italics Indicate the AIRS Radiance Data With Different Methods, AIRS (GSI clr) Uses the AIRS-Alone Cloud Detection, AIRS (MOD clr) Are AIRS/MODIS Cloud Detection, and AIRS (MOD cld-clr) Is the AIRS/MODIS Cloud-Clearing Method)

Experiment	GTS	AMSU-A	AIRS (GSI clr)	AIRS (MOD clr)	AIRS (MOD cld-clr)
GTS + AMSU-A + AIRS (GSI clr)	Yes	Yes	Yes		
GTS + AMSU-A + AIRS (MOD clr)	Yes	Yes		Yes	
GTS + AMSU-A + AIRS (MOD cld-clr)	Yes	Yes			Yes

for various research purposes. The physical schemes in this work are listed in section 3.4. WRF-ARW is used in daily runs for regional NWP short-term forecasts, such as NCEP Rapid Refresh and SDAT.

3.4. Data and Experiments

Data from the World Meteorological Organization's Global Telecommunication System (GTS), AMSU-A, and AIRS (Table 1) are used in this study. GTS includes all the conventional data, such as surface observations, radiosondes, wind profile, aircraft data, etc. AMSU-A includes observations made by AQUA, Metop-A, NOAA-15, and NOAA-18. Three different types of AIRS radiances are tested. The AIRS (GSI clr) provides the AIRS radiances using the GSI stand-alone cloud detection method; the AIRS (MOD clr) provides the AIRS radiances using collocated high spatial resolution MODIS cloud mask for sounder subpixel cloud detection; and the AIRS (MOD cld-clr) is the AIRS clear radiances using MODIS for sounder subpixel cloud detection plus the AIRS/MODIS cloud-cleared radiances. To avoid the complexity of land surface (i.e., emissivity), only AIRS cloud-cleared radiances over ocean are used in the assimilation experiments. The thinning mesh is 60 km for AMSU-A and 120 km for AIRS. The background error covariance matrix and observation error table used in GSI follows the NCEP operational system, i.e., North American Mesoscale Forecast System [*McCarty et al*., 2009].

Based on *Goldberg et al*. [2003], 281 channels of AIRS data are selected for NWP centers. But not all of the 281 channels of AIRS are used in the GSI system. Due to the local thermal equilibrium effects, large innovation differences, and dominated penalty function, 152 channels are selected from the 281 channels based on the NCEP operational center [*Jung*, 2008]. Besides, the channels located in the shortwave spectrum and those with significant ozone absorption are also rejected in the regional assimilation. Combining the NCEP operational and the regional model channel selections, there are 120 channels assimilated in the GSI in this study (Figure 2). The surface channel assimilation follows the same schemes as demonstrated by *Lim et al*. [2014]. All three experiments used the same set of AIRS channels. The bias correction has two parts: air mass bias and satellite scan dependent bias. In this study, the initial bias coefficients are from the NCEP Global Forecast System. The air mass bias correction coefficient is updated based on the previous results for each cycling run. Therefore, the bias correction coefficients of the three experiments are different.

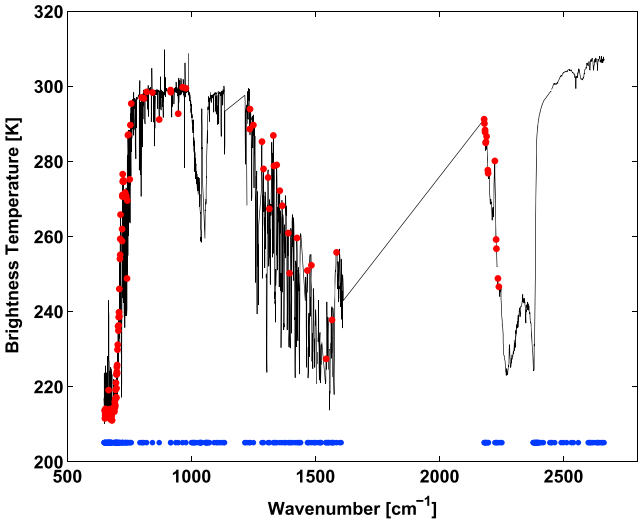

Figure 2. An example of AIRS spectrum (black) and the corresponding 281 channels (blue dots) selected for the NWP center. The red dots are the selected 120 channels from 281 channels that were assimilated in this study.

For the Hurricane Sandy experiments, the assimilation time is from 1800 UTC 25 October to 0000 UTC 27 October at every 6 h cycle with a ±1.5 h assimilation window. A 72 h forecast, from 1800 UTC 28 October to 0000 UTC 30 October 2012, followed. The experiments for Hurricanes Irene and Ike are similar to those for Hurricane Sandy. The assimilation time for Irene is from 1200 UTC 22 August to 0000 UTC 24 August. The forecast time was

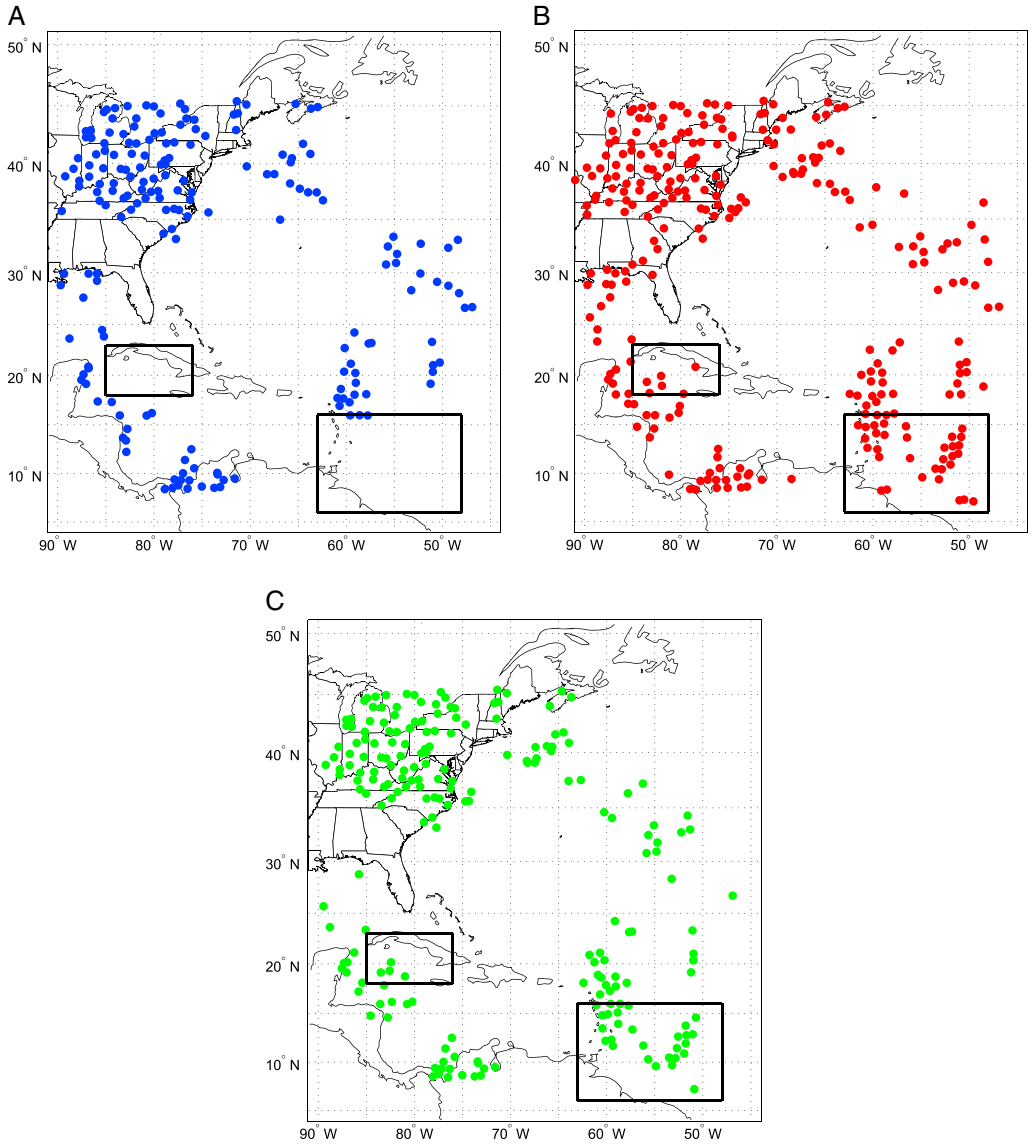

Figure 3. The locations at 1800 UTC 25 October 2012 for Hurricane Sandy where AIRS channel 210 (709.5659 cm^{-1}) is assimilated in the GSI for AIRS (GSI clr) (lower left red), AIRS (MOD clr) (upper blue), and AIRS (MOD cld-clr) (lower right green).

run from 1200 UTC 25 August to 0000 UTC 27 August 2011. The assimilation time for Hurricane Ike is from 1800 UTC 5 September to 0000 UTC 7 September, and the forecast time is from 1800 UTC 5 September to 0000 UTC 10 September 2008.

The horizontal resolution for the experiments is 12 km with 400 × 350 grid points, and the vertical is from the surface to 10 hPa instead of the default 50 hPa. The analysis domain is described in *Wang et al.* [2014]. The microphysics scheme used is the WRF Single-Moment six-class scheme by *Hong and Lim* [2006]. Longwave and shortwave radiation schemes used are the Rapid Radiative Transfer Model for global applications (RRTMG) scheme [*Iacono et al.*, 2008]. The planetary boundary layer is the Yonsei University scheme (YSU) [*Hong et al.*, 2006], and the cumulus parameterization option is the Kain-Fritsch scheme [*Kain*, 2004].

Three experiments are carried out to demonstrate the impact of the AIRS cloud-cleared radiances assimilation (Table 1): GTS + AMSU-A + AIRS (GSI clr) or AIRS (GSI clr) for simplicity, GTS + AMSU-A + AIRS (MOD clr) or AIRS (MOD clr), and GTS + AMSU-A + AIRS (MOD cld-clr) or AIRS (MOD cld-clr). All three experiments assimilate GTS, AMSU-A radiances, and AIRS radiances. The differences are the AIRS radiances: GSI clr uses GSI stand-alone cloud detection for AIRS clear radiances, MOD clr uses collocated

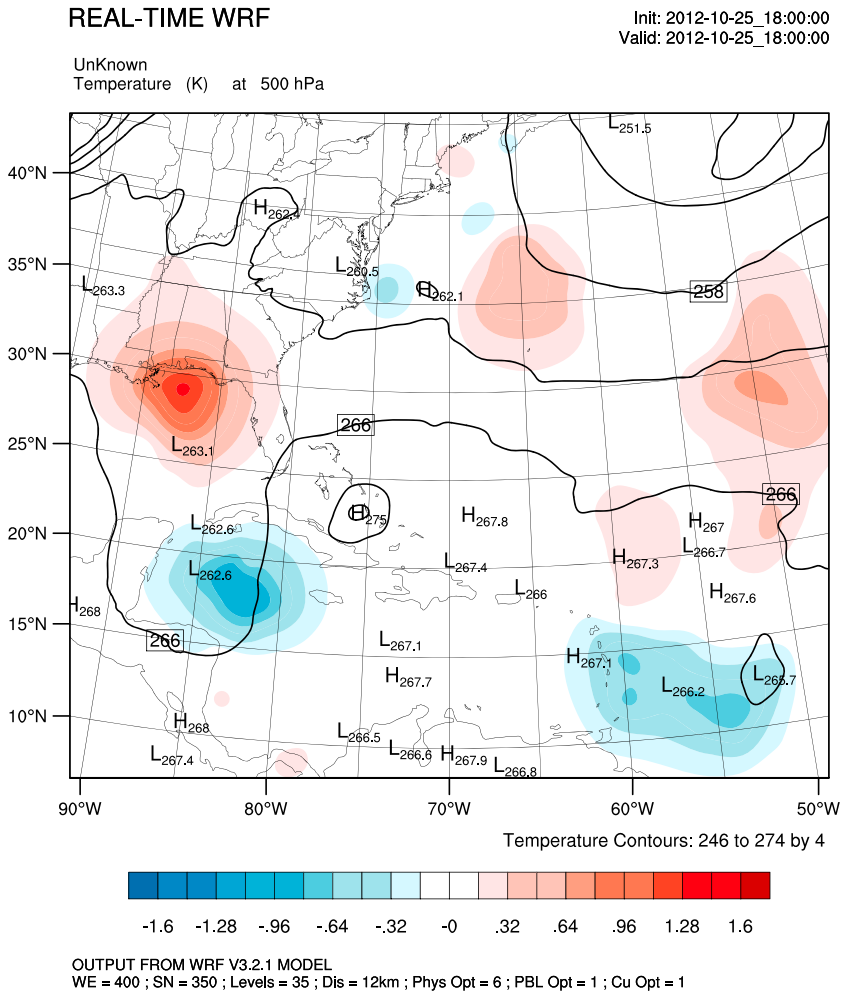

Figure 4. The difference in temperature (shaded, unit: K) analysis between AIRS (MOD cld-clr) and AIRS (MOD clr) with temperature (contour, unit: K) of AIRS (MOD cld-clr) at 500 hPa at 1800 UTC 25 October 2012 for Hurricane Sandy.

MODIS cloud mask for AIRS clear radiances, and MOD cld-clr uses MODIS cloud mask for AIRS clear radiances and AIRS/MODIS cloud clearing for additional AIRS clear equivalent radiances. The comparison between AIRS (GSI clr) assimilation and AIRS (MOD clr) assimilation was discussed in *Wang et al.* [2014]. The following sections in this study investigate the impact from additional cloud-cleared AIRS radiances on hurricane forecasts, and the results of AIRS (GSI clr) assimilation are used as reference in the following discussions.

4. Influences on Analysis Fields

4.1. Coverage of AIRS Radiances

The number and quality of observations highly affected the data assimilation. Better quality observations usually lead to better analysis/forecast. On the other hand, poor quality observations, even a small percentage, can cause significant negative impacts on the analysis and forecast. The coverage of AIRS radiances assimilated in the GSI at 1800 UTC 25 October 2012 is shown in Figure 3 for AIRS channel 210 (709.5659 cm^{-1}). The weighting function of this channel peaks near 500 hPa. The number of assimilated observations is 283 for AIRS (GSI clr), 186 for AIRS (MOD clr), and 211 for AIRS (MOD cld-clr). With more accurate cloud detection using the MODIS high spatial resolution cloud mask product [*Ackerman et. al.*, 1998; *Ackerman et. al.*, 2008], the number of AIRS (MOD clr) assimilated radiances is smaller than with the GSI stand-alone cloud detection, which greatly reduces the possibility of cloud contamination.

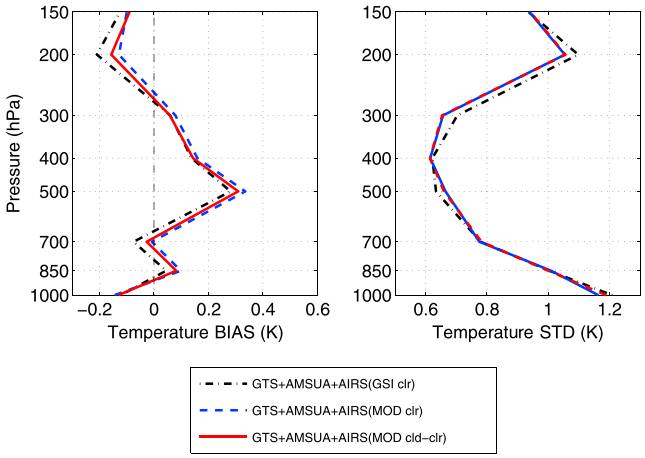

Figure 5. Temperature (left) BIAS and (right) SD are from radiosonde minus AIRS (GSI clr) (dash dot black, unit: K), AIRS (MOD clr) (solid blue, unit: K), and AIRS (MOD cld-clr) (dashed red, unit: K) at analysis time for Hurricane Sandy.

Comparing AIRS (GSI clr) and AIRS (MOD clr), some mismatches are found in the Caribbean Sea and south of the North Atlantic Ocean. The mismatched regions are cloudy regions according to the MODIS cloud mask, but deemed clear sky by the stand-alone cloud detection in GSI. This can potentially cause biases in the analysis fields. The black rectangles (Figure 3) show that the number of observations is increased in partially cloudy regions by assimilating the cloud-cleared radiances, which were rejected by AIRS (MOD clr) but accepted by AIRS (GSI clr). More data are assimilated in AIRS (MOD cld-clr) than in AIRS (clr), because the cloud-clearing method generates AIRS clear equivalent radiances for assimilation in some partially cloudy regions. These additional cloud-cleared radiances increase the number of observations that are assimilated by GSI, with expected gains on the quality of analyses and forecasts.

4.2. Analysis Fields of Temperature

The assimilation of advanced IR radiances provides the atmospheric thermodynamic information for improving NWP initialization. Impact on the initialization (or the analysis fields), due to different methods of assimilating AIRS radiances, is analyzed below.

The temperature analysis field and the difference between AIRS (MOD cld-clr) and AIRS (MOD clr) at 1800 UTC on 25 October 2012 are shown in Figure 4. The cloud-clearing method extracts the radiance arising from the clear air portion of partly cloudy FOVs to represent the thermodynamic information in partially cloudy regions. It is therefore expected that the analysis with the assimilation of cloud-cleared radiances is warmer than that with the cloud-contaminated clear radiances from the GSI stand-alone cloud detection. The region over Florida is one such example. However, there are regions over the Caribbean Sea and south of the North Atlantic Ocean in Figure 4 showing the opposite. Careful examination of the MODIS cloud mask reveals that these regions have no clear radiances. As a result, there is thermodynamic information from AIRS (MOD clr) impacted background. From the differences plot shown in Figure 4, the warmer background in those regions is decreased more from the assimilation of AIRS (MOD cld-clr) compared with that from the assimilation of AIRS (MOD clr).

4.3. Comparing the Analysis Temperature Profiles With Radiosondes

Temperature profiles are extracted from the analyses and compared with the radiosondes valid at the analysis time. Temperature BIAS (radiosondes minus the analysis profiles) and SD (standard deviation) between the analysis profiles and radiosondes are shown in Figure 5. Approximately 200 radiosondes profiles located within the model domain are used for verification of the analysis filed. The number of radiosondes observations varied with pressure levels (Table 2). Figure 6 shows an example of the radiosondes locations at 0000 UTC on 26 October, 2012. Approximately 30–35 radiosondes are present at one time period on each pressure level. The six experiments taken together make the sum of radiosondes between 200 and 222.

From Figure 5, temperature BIAS ranges from −0.2 K to 0.33 K. For temperature BIAS, there are obvious differences among the three: the AIRS (GSI clr) appears to have a slightly smaller bias compared with AIRS (MOD clr) and AIRS (MOD cld-clr) between 300 and 850 hPa; the AIRS (MOD cld-clr) appears to have a slightly smaller bias than AIRS (MOD clr). For temperature root-mean-square error (RMSE), there are little differences between AIRS (MOD clr) and AIRS (MOD cld-clr), both have slightly smaller RMSE than AIRS (GSI clr) except around 600 hPa. These results indicate that the MODIS cloud detection and the cloud clearing

Table 2. The Number of Radiosondes at Different Pressure Levels From 1000 hPa to 150 hPa for Hurricane Sandy

Levels (hPa)	1000	850	700	500	400	300	200	150
Analysis time	137	221	217	218	215	214	214	214
24 h forecast	149	223	221	220	219	219	215	217
48 h forecast	135	223	222	223	224	220	217	218
72 h forecast	105	221	222	222	222	220	217	218

have impacts on the analysis temperature field. However, the impacts are so subtle that no single experiment is significantly better than the other two. Although comparisons with radiosondes in all three types of analysis are very similar, it can be seen in next section that impacts on forecasts are quite different.

5. Influence on Forecasts

5.1. Analyzing Forecast Fields on Hurricane Track

Large-scale circulation affects the tropical cyclone track, especially due to the different large-scale patterns [*Harr and Neumann*, 1991; *Harr and Elsberry*, 1993; *Lander*, 1995]. The differences between large-scale patterns of AIRS (MOD clr) and AIRS (MOD cld-clr) are discussed in this section, and the impacts on the track forecast are shown. Figure 7 shows the temperature and geopotential height after the 72 h forecast on AIRS (MOD cld-clr) at 850 hPa and differences between AIRS (MOD cld-clr) and AIRS (MOD clr) (AIRS (MOD cld-clr) minus AIRS (MOD clr)). The difference in temperature between AIRS (MOD cld-clr) and AIRS (MOD clr) shows that AIRS (MOD cld-clr) is warmer southeast of the hurricane center and colder northwest of the hurricane center. The difference in geopotential height shows that AIRS (MOD cld-clr) is lower southeast of the hurricane center and higher northwest of the hurricane center. AIRS (MOD cld-clr) minus AIRS (GSI clr) shows a similar pattern. Based on the potential tendency equation [*Holton*, 2004], for the region where the temperature is warmer than the surroundings, the geopotential height at the same pressure level is lower; where the temperature is colder than the surroundings, the geopotential height is higher. A mature hurricane has a minimum sea level pressure center with a warm-core structure [*Ooyama*, 1969; *Kurihara and Tuleya*, 1974; *Merrill*, 1988]. The warmer temperature and lower geopotential height region of AIRS (MOD cld-clr) is further southeast compared to AIRS (MOD clr) and AIRS (GSI clr). This difference indicates the hurricane center of AIRS (MOD cld-clr) is southeast of the hurricane center of AIRS (MOD clr) and AIRS (GSI clr). Comparing the 72 h hurricane tracks and the best track from National Hurricane Center (NHC) (see the bottom of Figure 5), at 1800 UTC on 29 October, the hurricane center of AIRS (MOD cld-clr) is southeast of the hurricane center of AIRS (MOD clr) and AIRS (GSI clr). The track of AIRS (MOD cld-clr) near the 72 h forecast is much better by more than 50 km than the other two forecasts.

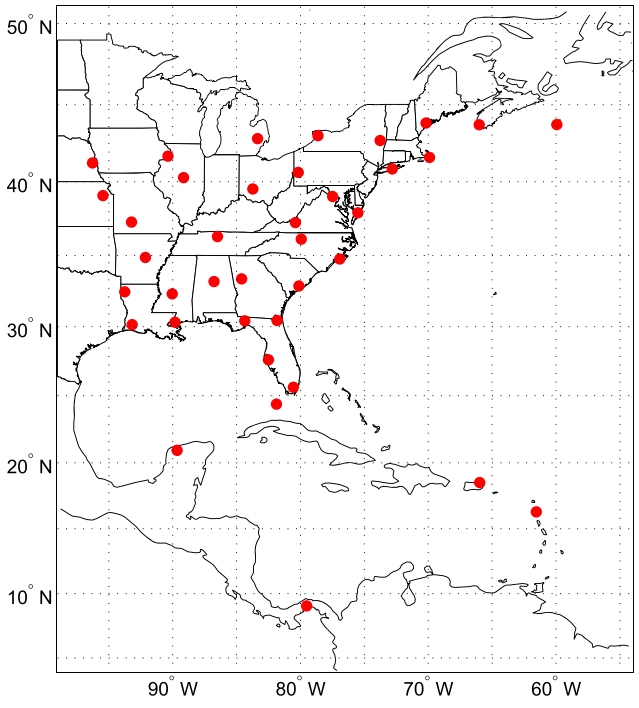

Figure 6. The locations of radiosondes are used to compare with analysis fields at 0000 UTC 26 October 2012.

5.2. Comparison With GOES-13 Imager Brightness Temperature Observations

The 11 μm simulated brightness temperature of the 72 h forecast is compared with the observations from the GOES-13 imager channel 4 at 1800 UTC 28

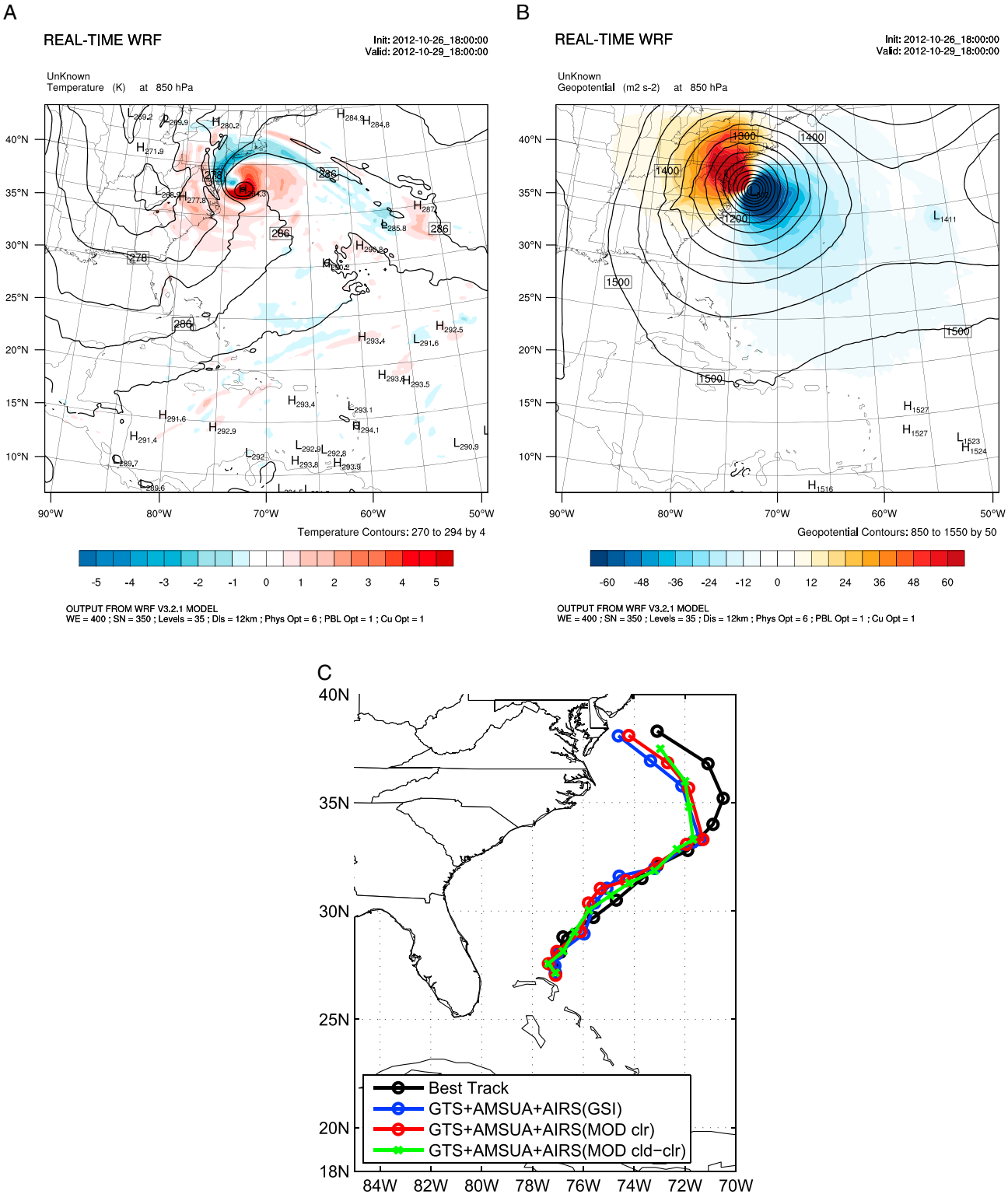

Figure 7. The difference in (a) temperature (upper left shaded, unit: K) and (b) geopotential height (upper right shaded, unit: m) at the 72 h forecast between AIRS (MOD cld-clr) and AIRS (MOD clr) (AIRS (MOD cld-clr) minus AIRS (MOD clr)) with temperature (upper left contour) and geopotential height (upper right contour) of AIRS (MOD cld-clr) at 850 hPa at 1800 UTC 29 October 2012. (c) Hurricane Sandy tracks for a 72 h forecast from 1800 UTC 26 October to 1800 UTC 29 October 2012.

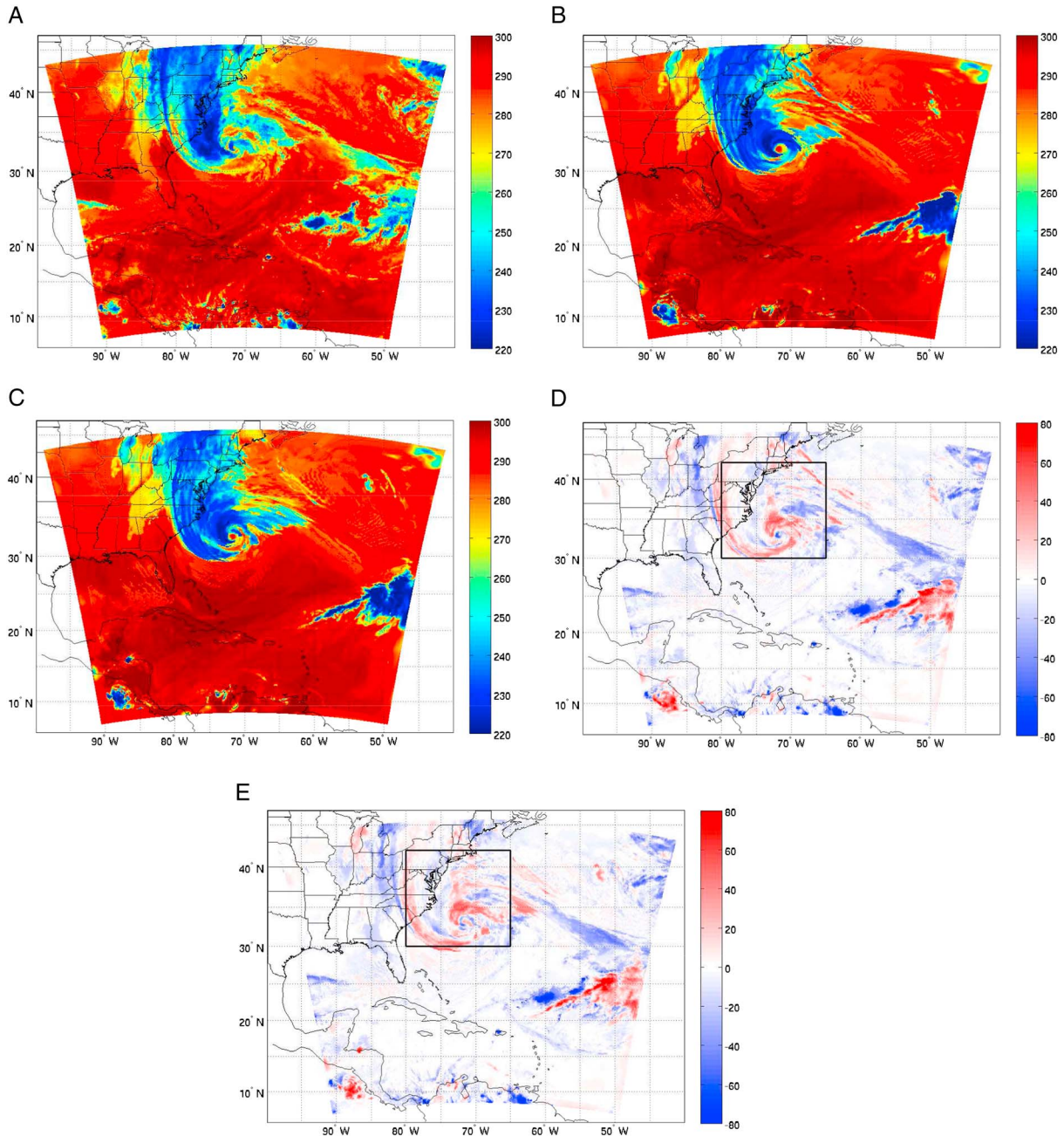

Figure 8. The brightness temperature of GOES-13 channel 4 (11 μm) observations (top, unit: K), simulated 72 h forecast brightness temperature of AIRS (MOD clr) (middle left) and AIRS (MOD cld-clr) (middle right), the difference of brightness temperature between observations and AIRS (MOD clr) (bottom left) and between observations and AIRS (MOD cld-clr) (bottom right) at 1800 UTC 28 October 2012.

October 2012 (Figure 8). The Pressure-Layer Fast Algorithm for Atmospheric Transmittance (PFAAST) model [*Hannon et al.*, 1996; *Li et al.*, 2009] is used as the radiative transfer model to calculate the clear-sky GOES 13 radiances. The cloudy radiances are calculated by coupling the clear-sky optical thickness from PFAAST with the cloud optical thickness (COT) at 0.55 μm, which is calculated using a fast radiative transfer cloud model developed by the University of Wisconsin-Madison (UW) and Texas A&M University [*Baum et al.*, 2000; *Wei et al.*, 2004]. For ice clouds, COT is calculated from the ice water path [*Heymsfield et al.*, 2003]; and for water clouds, the cloud droplet is assumed to be spherical and the classical Lorenz-Mie theory is used to calculate the single-scattering properties.

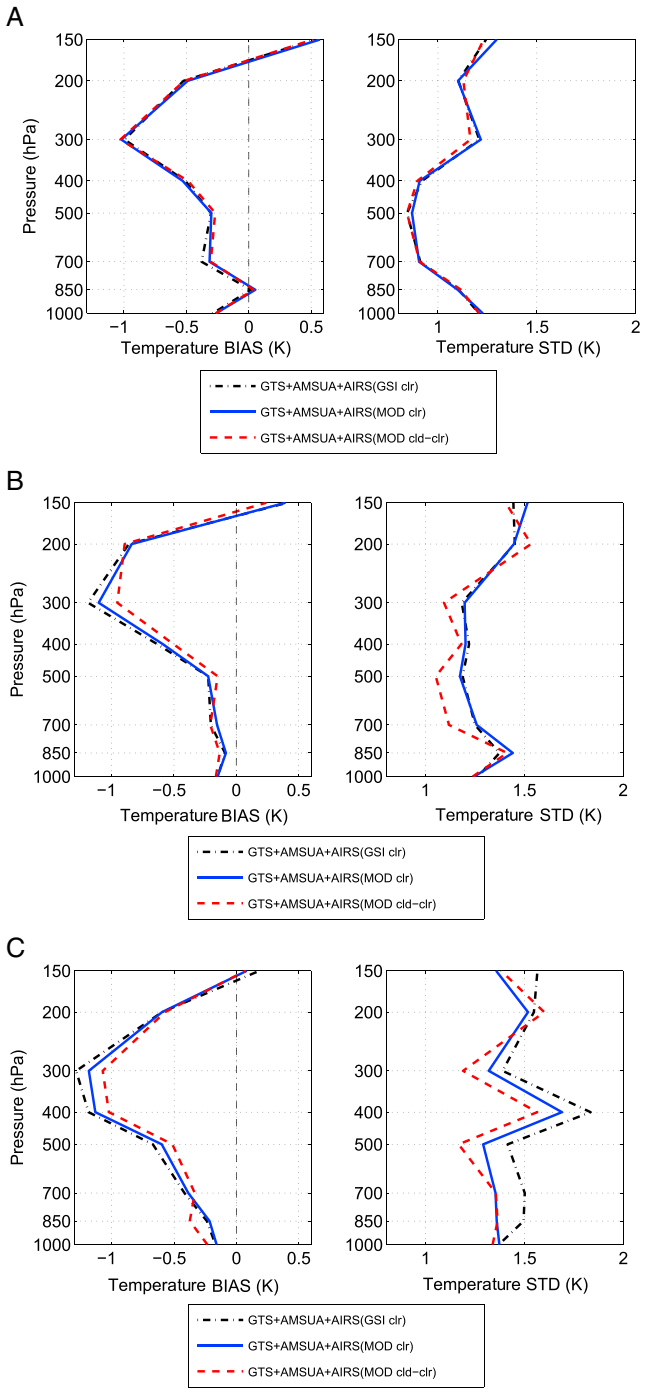

Figure 9. (a–c, left column) BIAS and (a–c, right column) SD for 24 h forecasts (Figure 9a, left and right), 48 h forecasts (Figure 9b, left and right), and 72 h forecasts (Figure 9c, left and right) of temperature profiles between the AIRS (GSI clr) (dash-dot black, unit: K) and radiosondes, AIRS (MOD clr) (solid blue line, unit: K) and radiosondes, and AIRS (MOD cld-clr) (dashed red line, unit: K) and radiosondes from 1000 hPa to 150 hPa for Hurricane Sandy.

At 1800 UTC 28 October, Hurricane Sandy passed southeast of North Carolina, with cold clouds (brightness temperature (BT) around 230 K) northwest of the hurricane center, and relatively few clouds and a warm area (BT around 280 K) southeast of the hurricane center. Comparing the simulated GOES-13 Imager brightness temperature from AIRS (MOD clr) and AIRS (MOD cld-clr), substantial differences are seen around the hurricane center (Figure 6, bottom). The brightness temperature from AIRS (MOD cld-clr) better reflects the curly structure of the clouds around the hurricane center, and the relatively few clouds and warm area southeast of the center. Quantitatively, this can be verified using the standard deviation of the difference (SD) of brightness temperature between the observations and the simulations. For the whole domain, the SD is 13.78 K from AIRS (MOD clr) and 13.77 K from the AIRS (MOD cld-clr). If we focus on the region of hurricane center (black box in Figure 6, bottom), the SDs are 17.29 K from AIRS (MOD clr) and 17.15 K from AIRS (MOD cld-clr). These results indicate that the assimilation of AIRS (MOD cld-clr) generates radiances closer to GOES-13 Imager than AIRS (MOD clr).

5.3. Forecasts Validation With Radiosondes

Radiosondes could also be used to validate the performance of the forecasts fields. The temperature profiles are extracted from the forecasts. Temperature BIAS (radiosondes minus the temperature of the forecast fields) and SD at 24 h, 48 h and 72 h forecast times are shown in Figure 9. The number of radiosonde profiles used differs with the pressure levels (Table 2). An example map of the radiosonde sites at one time period is shown in Figure 5. More than half of the stations are near the coast. Both the stations near the coast and over the continental US (CONUS) could be used to verify the improvements of the forecast fields with assimilation of AIRS (MOD clr) and AIRS (MOD cld-clr), respectively, over that with the assimilation of AIRS (GSI clr). From the 24 h forecast to the 72 h forecast, AIRS (MOD cld-clr) shows a

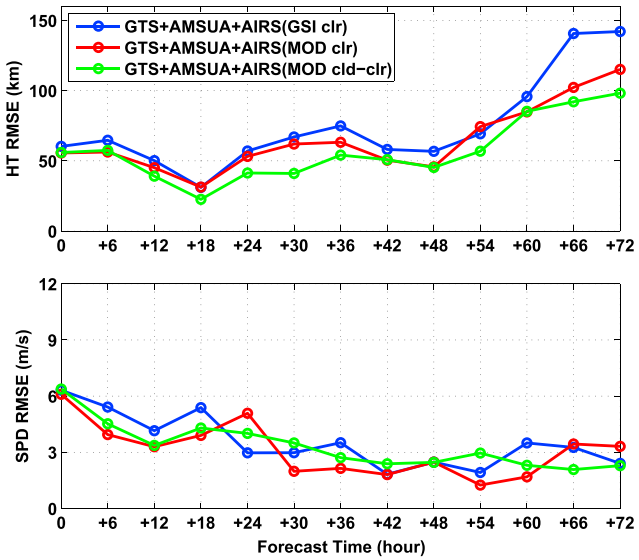

Figure 10. The (top) track and (bottom) maximum wind speed forecast RMSE with AIRS (GSI clr) (blue), AIRS (MOD clr) (red), and AIRS (MOD cld-clr) (green). Data are assimilated every 6 h from 18 UTC on 25 October to 00 UTC on 27 October 2012, followed by 72 h forecasts for Hurricane Sandy (2012).

consistent improvement over AIRS (MOD clr) and AIRS (GSI clr). At the 24 h forecast time, the differences of temperature BIAS among the three experiments are small (less than 0.1 K). Around 300 hPa, the forecast BIAS is around 1 K in absolute value, which is larger than the atmosphere beneath where the BIAS is mostly less than 0.5 K. This is likely due to the model simulation error near the tropopause. At the 48 h forecast time, the differences among the three experiments become more substantial. The AIRS (MOD cld-clr) shows substantial improvements over AIRS (GSI clr) and AIRS (MOD clr). The BIAS of AIRS (MOD cld-clr) at 300 hPa is about 0.08 K smaller than AIRS (GSI clr) and 0.1 K smaller than AIRS (MOD clr).

An average improvement of 0.1 K in SD is also evident between 250 and 750 hPa. AIRS (MOD clr) and AIRS (GSI clr) show similar performance. At the 72 h forecast time, the improvement from AIRS (MOD cld-clr) becomes more profound. The average improvement between 250 and 700 hPa is 0.25 K over AIRS (GSI clr) and 0.2 K over AIRS (MOD clr). Similar improvements are seen in the RMSE. It is important to point out that the AIRS (MOD clr) has slight improvements over MOD (GSI clr), which is consistent with *Wang et al*. [2014].

For Hurricane Irene, similar results are seen when comparing forecast temperatures with radiosondes. The BIAS of the forecast temperature with AIRS (MOD cld-clr) assimilation is about 0.05 K smaller than that of AIRS (MOD clr). These results indicate that the extra cloud-cleared AIRS radiances provide positive impacts for the temperature forecast.

5.4. Hurricane Track Error and Intensity Error

Hurricane forecast are validated against the actual storm track and its intensity with time (the best track and observations data were obtained from NOAA's NHC). Intensity is a measure of extreme meteorological conditions, either the maximum sustained (low-level) wind or the minimum sea level pressure is used [*Merrill*, 1988]. Figure 10 shows the RMSE of the hurricane track (top) and maximum wind speed (bottom) of the 72 h forecasts for Hurricane Sandy. The RMSE of the hurricane track from AIRS (MOD cld-clr) is the smallest among the three experiments for the entire time period, especially after the 18 h forecasts. The RMSE of the hurricane track from AIRS (MOD clr) is 10 to 25 km smaller than

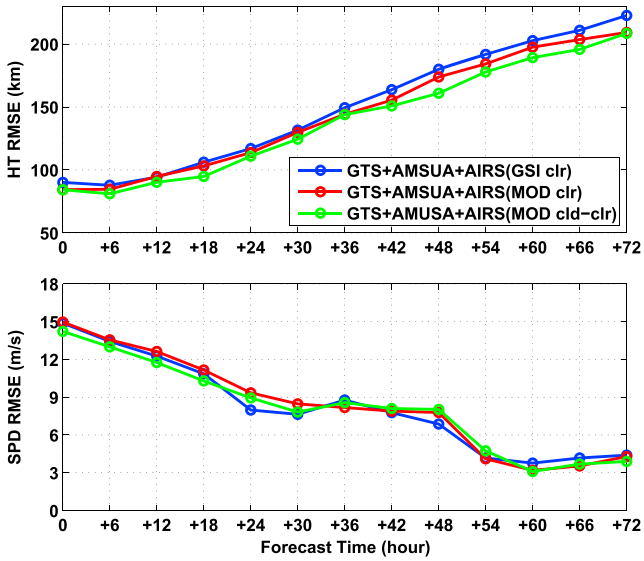

Figure 11. The same as Figure 10 but for Hurricane Irene.

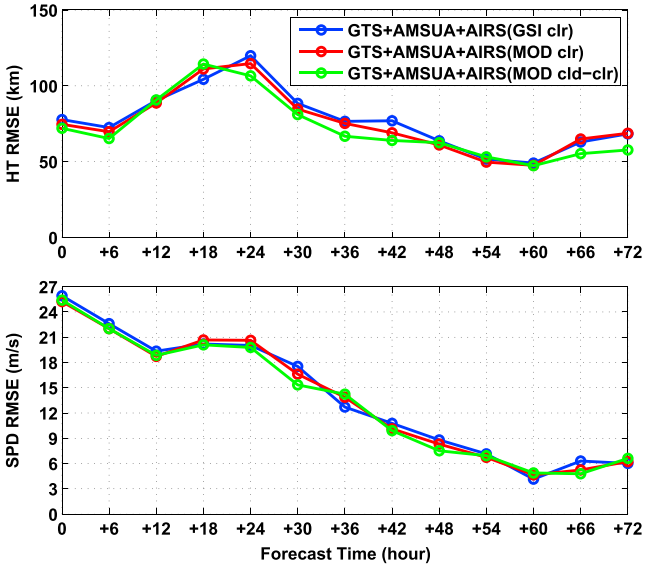

Figure 12. The same as Figure 10 but for Hurricane Ike (2008).

that from AIRS (MOD clr), and 10 to 50 km smaller than that from AIRS (GSI clr). For the maximum wind speed, the three experiments have comparable results, making it difficult to determine which is better. The RMSE of the hurricane track for Hurricane Irene (Figure 11, top) shows similar results with AIRS (MOD cld-clr) having the smallest track error compared to AIRS (MOD clr) and AIRS (GSI clr), especially after 36 h forecasts. For the maximum wind speed prediction, it is neutral for all three experiments. For Hurricane Ike (Figure 12), the RMSE of the hurricane track also shows that the assimilation of the AIRS (MOD cld-clr) improves the track error by approximately 10 km compared to that of AIRS (MOD clr) and AIRS (GSI clr). The maximum wind speed prediction of Hurricane Ike with the assimilation of AIRS (MOD cld-clr) gives slightly smaller errors compared to (GSI clr).

It is interesting that the assimilation of AIRS (MOD clr and MOD cld-clr) radiances provides positive impacts on hurricane track but neutral impacts on hurricane intensity. Possible reason for this could be because of the limited penetration capability of IR radiances. Both AIRS (GSI clr) and AIRS (MOD clr) assimilate clear radiances, which mostly come from the environmental region and contain little information about the cloudy region (i.e., hurricane). Even though cloud-clearing techniques extract clear-sky radiances from a cloudy FOV, which contain information within and below the clouds, it works better for partly cloudy FOVs, which still account for the environment.

6. Summary

Direct assimilation of cloudy radiances will continue to be challenging before we can link more adequately model cloud parameters and equivalent radiance observations. This study provides an alternative way to assimilate thermodynamic information in cloudy regions by taking advantage of a collocated high spatial resolution imager and advanced IR sounder on board the same platform. By having collocated high spatial resolution imager measurements, advanced IR sounder subpixel cloud characterization, cloud clearing, and quality control make it possible for effective assimilation of thermodynamic information in cloudy skies. Since the cloud-clearing method retrieves clear equivalent radiances, the same clear radiance assimilation approach can be applied directly to the cloud-cleared radiances. Therefore, the assimilation of thermodynamic information in cloudy skies is not limited by the uncertainty of the cloudy radiative transfer model. Our study with Hurricanes Sandy, Irene, and Ike shows that assimilating cloud-cleared AIRS radiances in cloudy skies reduces the SD of the temperature difference between the 72 h forecast and radiosondes by approximately 0.3 K compared to assimilating AIRS (GSI) clear radiances. The track forecasts are substantially improved by 10 to 50 km, compared to only clear radiance assimilation. The intensity forecast has neutral impact, possibly due to limited penetration capability of the IR radiances. A complementary data set could be microwave radiance observations. In the cloud-clearing method, the accuracy of the cloud-cleared radiances highly depends on the uniformity of the atmosphere, surface, cloud geometric, and optical properties (known as "scene uniformity") across the FOVs. Uniformity occurs more over ocean than over land, thus imager/sounder cloud clearing provides a way for indirect assimilation of thermodynamic information in cloudy regions, especially for TC forecasts over oceans. Since a minimum of two FOVs is required for extrapolation, the cloud-clearing process reduces the spatial resolution of the original observations. Theoretically, it is much more complicated to require more than two FOVs when clouds exist in the cloud-clearing domain. However, under these cases the valid

assumption of "scene uniformity" is less frequent and a reliable cloud-cleared solution is rare. Despite all of the shortcomings inherent in the cloud-clearing method, it remains as a possible way to potentially increase the yield of using some of the cloudy hyperspectral infrared data indirectly, as indicated by TC forecasts from Hurricane Sandy and Hurricane Irene with SDAT. The cloud-clearing technique can also be applied to Cross-track Infrared Sounder (CrIS)/Visible Infrared Imaging Radiometer and Infrared Atmospheric Sounding Interferometer/Advanced Very High Resolution Radiometer for radiance assimilation in NWP models. Future work includes comparison between cloud-cleared radiance assimilation and direct cloudy radiance assimilation, and the assimilation of hydrometric information in cloudy situations. Assimilation of CrIS/ATMS (advanced Technology Microwave Sounder) cloud-cleared radiances will also be tested in SDAT.

Acknowledgments

The authors would like to thank the three anonymous reviewers for the valuable suggestions and comments to improve the quality of this paper. This work is supported by JPSS Proving Ground and Risk Reduction (PGRR) and NOAA GOES-R high impact weather (HIW) (NA10NES4400013 and GYHY20140611). The views, opinions, and findings contained in this report are those of the authors and should not be construed as an official National Oceanic and Atmospheric Administration's or U.S. government's position, policy, or decision. We deeply appreciate CIMSS sounding team for providing the AIRS/MODIS cloud-cleared radiances and AIRS clear radiances with MODIS cloud detection. The hurricane observations are from National Hurricane Center. All the other data (GTS, AMSU-A, and AIRS) are publicly accessible from National Centers for Environmental Prediction/National Weather Service/NOAA/U.S. Department of Commerce (available from http://rda.ucar.edu/). All the models, algorithms, and experiments are conducted at NOAA/NESDIS-funded Supercomputer for Satellite Simulations and data assimilation Studies (S4) physically located at UW-Madison Space Science Engineering Center (SSEC).

References

Ackerman, S. A., K. I. Strabala, W. P. Menzel, R. A. Frey, C. C. Moeller, and L. E. Gumley (1998), Discriminating clear-sky from clouds with MODIS, *J. Geophys. Res.*, *103*(D24), 32,141–32,157, doi:10.1029/1998JD200032.

Ackerman, S. A., R. E. Holz, R. Frey, E. W. Eloranta, B. Maddux, and M. McGill (2008), Cloud detection with MODIS: Part II validation, *J. Atmos. Oceanic Technol.*, *25*, 1073–1086.

Auligné, T., F. Rabier, L. Lavanant, and M. Dahoui (2003), First results of the assimilation of AIRS data in Meteo-France numerical weather prediction model, in *Proceedings of the Thirteenth International TOVS Study Conference*, pp. 74–79, Sainte Adele, Canada.

Avila, L. A., and J. Cangialosi (2011), Hurricane Irene (AL092011) 21–28 August 2011, *Tropical Cyclone Rep.*, 1–45.

Baum, B. A., P. F. Soulen, K. I. Strabala, M. D. King, S. A. Ackerman, W. P. Menzel, and P. Yang (2000), Remote sensing of cloud properties using MODIS airborne simulator imagery during SUCCESS. II. Cloud thermodynamic phase, *J. Geophys. Res.*, *105*, 11,781–11,792, doi:10.1029/1999JD901090.

Berg, R. (2009), Hurricane Ike (AL092008) 1-14 September 2008, *Tropical Cyclone Rep.*, 1–55.

Blake, E. S., T. B. Kimberlain, R. J. Berg, J. P. Cangialosi, and J. L. Beven II (2013), Hurricane Sandy (AL182012) 22–29 October 2012, *Tropical Cyclone Rep.*, 1–157.

Cameron J., Collard A., English S. 2005, Operational use of AIRS observations at the Met Office, Tech. Proceedings 14th Internat. TOVS Study Conf., Beijing, China, 25–31 May 2005. [Available at: http://cimss.ssec.wisc.edu/itwg/itsc/itsc14.]

Cardinali, C. (2009), Forecast sensitivity to observation (FSO) as a diagnostic tool, ECMWF Research Department Technical Memorandum 599, ECMWF, Reading, U. K. [Available At http://old.ecmwf.int/publications/library/ecpublications/_pdf/tm/501600/tm599.pdf.]

Chen, Y., Y. Han, P. Van Delst, and F. Weng (2010), On water vapor Jacobian in fast radiative transfer model, *J. Geophys. Res.*, *115*, D12303, doi:10.1029/2009JD013379.

Chen, Y., Y. Han, and F. Weng (2012), Comparison of two transmittance algorithms in the community radiative transfer mode: Application to AVHRR, *J. Geophys. Res.*, *117*, D06206, doi:10.1029/2011JD016656.

English, S., J. Eyre, and J. Smith (1999), A cloud-detection scheme for use with satellite sounding radiances in the context of data assimilation for numerical weather predictions, *Q. J. Roy. Meteorol. Soc.*, *125*, 2359–2378.

Errico, R. M., P. Bauer, and J.-F. Mahfouf (2007), Issues regarding the assimilation of cloud and precipitation data, *J. Atmos. Sci.*, *64*, 785–3798, doi:10.1175/2006JAS2044.1.

Geer, A. J., and P. Bauer (2011), Observation errors in all-sky data assimilation, *Q. J. R. Meteorol. Soc.*, *137*, 2024–2037, doi:10.1002/qj.830.

Goldberg, M. D., Y. Qu, L. M. McMillin, W. Wolf, Z. Lihang, and M. Divakarla (2003), AIRS near-real-time products and algorithms in support of operational numerical weather prediction, *IEEE Trans. Geosci. Remote Sens.*, *41*(2), 379–389, doi:10.1109/TGRS.2002.808307.

Goldberg, M. D., T. S. King, W. W. Wolf, C. Barnet, H. Gu and L. Zhou (2005), Using MODIS with AIRS to develop an operational cloud-cleared radiance product, in *Proc. SPIE, Multispectral and Hyperspectral Remote Sensing Instruments and Applications II*, vol. 5655, edited by A. M. Larar, M. Suzuki, and Q. Tong, Honolulu, Hawaii, doi:10.1117/12.578824.

Han, Y., P. van Delst, Q. Liu, F. Weng, B. Yan, R. Treadon, and J. Derber (2006), JCSDA Community Radiative Transfer Model (CRTM)—Version 1, NOAA Tech. Rep. 122.

Hannon, S., L. L. Strow, and W. W. McMillan (1996), Atmospheric infrared fast transmittance models: A comparison of two approaches, *Proc. SPIE Int. Soc. Opt. Eng.*, *2830*, 94–105.

Harr, P. A., and R. L. Elsberry (1993), Variability of tropical cyclone track characteristics and large-scale circulation regimes over the western Pacific Ocean. Preprints, in *20th Conf. on Hurricanes and Tropical Meteorology*, pp. 97–100, Am. Meteorol. Soc., San Antonio, Tex.

Harr, P. A., and R. L. Neumann (1991), On the relative motion of binary tropical cyclones, *Mon. Weather Rev.*, *119*, 1448–1468.

Heilliette, S., and L. Garand (2007), A practical approach for the assimilation of cloudy infrared radiances and its evaluation using airs simulated observations, *Atmos.–Ocean*, *45*(4), 211–225, doi:10.3137/ao.450403.

Heymsfield, A. J., S. Matrosov, and B. Baum (2003), Ice water path-optical depth relationships for cirrus and deep stratiform ice cloud layers, *J. Appl. Meteorol.*, *42*, 1369–1390, doi:10.1175/1520-0450(2003)042<1369:IWPDRF>2.0.CO;2.

Holton, J. R. (2004), *An Introduction to Dynamic Meteorology*, 4th ed., pp. 157–159, Academic Press, San Francisco, Calif.

Hong, S.–Y., and J.-O. J. Lim (2006), The WRF single-moment 6-class microphysics scheme (WSM6), *J. Korean Meteorol. Soc.*, *42*, 129–151.

Hong, S.–Y., Y. Noh, and J. Dudhia (2006), A new vertical diffusion package with an explicit treatment of entrainment processes, *Mon. Weather Rev.*, *134*, 2318–2341, doi:10.1175/MWR3199.1.

Iacono, M. J., J. S. Delamere, E. J. Mlawer, M. W. Shephard, S. A. Clough, and W. D. Collins (2008), Radiative forcing by long-lived greenhouse gases: Calculations with the AER radiative transfer models, *J. Geophys. Res.*, *113*, D13103, doi:10.1029/2008JD009944.

Jung, J. A. (2008), The assimilation of hyperspectral satellite radiances in global numerical weather prediction, UMD theses and Dissertations. [Available at http://hdl.handle.net/1903/8166.]

Kain, J. S. (2004), The Kain-Fritsch convective parameterization: An update, *J. Appl. Meteorol.*, *43*, 170–181, doi:10.1175/1520-0450(2004)043<0170:TKCPAU>2.0.CO;2.

Kleist, D. T., D. F. Parrish, J. C. Derber, R. Treadon, W.–S. Wu, and S. Lord (2009), Introduction of the GSI into the NCEP global data assimilation system, *Weather Forecasting*, *24*, 1691–1705, doi:10.1175/2009WAF2222201.1.

Kurihara, Y., and R. E. Tuleya (1974), Structure of a tropical cyclone developed in a three-dimensional numerical simulation model, *J. Atmos. Sci.*, *31*, 893–919.

Lander, M. A. (1995), Specific tropical cyclone track types and unusual tropical cyclone motions associated with a reverse-oriented monsoon trough in the western North Pacific, *Weather Forecasting*, *11*, 170–186.

Le Marshall, J., et al. (2005a), AIRS hyperspectral data improves Southern Hemisphere forecasts, *Aust. Meteorol. Mag.*, *54*, 57–60.
Le Marshall, J., et al. (2005b), Impact of atmospheric infrared sounder observations on weather forecasts, *Eos Trans. AGU*, *86*(11).
Le Marshall, J., et al. (2006), Improving global analysis and forecasting with AIRS, *Bull. Am. Meteorol. Soc.*, *87*, 891–894.
Li, J., W. P. Menzel, F. Sun, T. J. Schmit, and J. Gurka (2004), AIRS subpixel cloud characterization using MODIS cloud products, *J. Appl. Meteorol.*, *43*, 1083–1094, doi:10.1175/1520-0450(2004)043<1083:ASCCUM>2.0.CO;2.
Li, J., C. Y. Liu, H.-L. Huang, T. J. Schmit, W. P. Menzel, and J. Gurka (2005), Optimal cloud-clearing for AIRS radiances using MODIS, *IEEE Trans. Geosci. Remote Sens.*, *43*, 1266–1278.
Li, J., J. Li, and P. Wang (2014), A near real-time regional satellite data assimilation system for high impact weather research and forecasts, *JCSDA Quarterly*, *46*, 1–5.
Li, Z., J. Li, W. P. Menzel, J. P. Nelson III, T. J. Schmit, E. Weisz, and S. A. Ackerman (2009), Forecasting and nowcasting improvement in cloudy regions with high temporal GOES sounder infrared radiance measurements, *J. Geophys. Res.*, *114*, D09216, doi:10.1029/2008JD010596.
Lim, A. H. N., J. A. Jung, H.-L. A. Huang, S. A. Ackerman, and J. A. Otkin (2014), Assimilation of clear sky atmospheric infrared sounder radiances in short-term regional forecasts using community models, *J. Appl. Rem. Sens.*, *8*, 083655–1–083655–27, doi:10.1117/1.JRS.8.083655.
McCarty, W., G. Jedlovec, and T. L. Miller (2009), Impact of the assimilation of Atmospheric Infrared Sounder radiance measurements on short-term weather forecasts, *J. Geophys. Res.*, *114*, D18122, doi:10.1029/2008JD011626.
McNally, A. P., and P. D. Watts (2003), A cloud detection algorithm for high-spectral-resolution infrared sounders, *Q. J. R. Meteorol. Soc.*, *129*, 3411–3423, doi:10.1256/qj.02.208.
McNally, A. P., P. D. Watts, J. A. Smith, R. Engelen, G. A. Kelly, J. N. Thépaut, and M. Matricardi (2006), The assimilation of AIRS radiance data at ECMWF, *Q. J. R. Meteorol. Soc.*, *132*, 935–957, doi:10.1256/qj.04.171.
Merrill, R. T. (1988), Environmental influences on hurricane intensification, *J. Atmos. Sci.*, *45*, 1678–1687, doi:10.1175/15200469(1988)045<1678:EIOHI>2.0.CO;2.
Nagle, F. W., and R. E. Holz (2009), Computationally efficient methods of collocating satellite, aircraft, and ground observations, *J. Atmos. Oceanic Technol.*, *26*, 1585–1595.
Okamoto, K., H. Owada, T. Egawa, and T. Ishibashi (2008), Assimilation of radiance data at JMA: Recent developments and prospective plans, *Proc. of the 16th Int. TOVS Study Conf.*, Angra dos Reis, Brazil, 7–13 May.
Ooyama, K. (1969), Numerical simulation of the life cycle of tropical cyclones, *J. Atmos. Sci.*, *26*, 3–40.
Pangaud, T., N. Fourrie, V. Guidard, M. Dahoui, and F. Rabier (2009), Assimilation of AIRS radiances affected by mid- to low-level clouds, *Mon. Weather Rev.*, *137*, 4276–4292, doi:10.1175/2009MWR3020.1.
Pavelin, E. G., S. J. English, and J. R. Eyre (2008), The assimilation of cloud-affected infrared satellite radiances for numerical weather prediction, *Q. J. R. Meteorol. Soc.*, *134*, 737–749.
Rienecker, M., R. Galaro, R. Todling, E. Liu, R. Errico, I. Stajner, M. Sienkiewicz, and R. Reichle (2008), GMAO's atmospheric data assimilation contributions to the JCSDA and future plans, JCSDA Seminar, 16 April 2008. [Available at http://www.jcsda.noaa.gov/documents/seminardocs/GMAO_JCSDA_20080416.pdf.]
Schwartz, C. S., Z. Liu, H.-C. Lin, and S. A. McKeen (2012), Simultaneous three-dimensional variational assimilation of surface fine particulate matter and MODIS aerosol optical depth, *J. Geophys. Res.*, *117*, D13202, doi:10.1029/2011JD017383.
Skamarock, W. C., J. B. Klemp, J. Dudhia, D. O. Gill, D. M. Barker, M. G. Duda, X.-Y. Huang, W. Wang, and J. G. Powers (2008), A description of the advanced research WRF version 3, NCAR Tech. Note, 1–113.
Smith, W. L., et al. (2004), Extraction of profile information from cloud contaminated radiances, *Proc. ECMWF Workshop on Assimilation of High Spectral Resolution Sounder in NWP*, pp. 145–154.
Stengel, M., M. Lindskog, P. Undén, and N. Gustafsson (2013), The impact of cloud-affected IR radiances on forecast accuracy of a limited-area NWP model, *Q. J. R. Meteorol. Soc.*, *139*, 2081–2096, doi:10.1002/qj.2102.
Wang, P., J. Li, J. Li, Z. Li, T. J. Schmit, and W. Bai (2014), Advanced infrared sounder subpixel cloud detection with imagers and its impact on radiance assimilation in NWP, *Geophys. Res. Lett.*, *41*, 1773–1780, doi:10.1002/2013GL059067.
Wei, H., P. Yang, J. Li, B. B. Baum, H.-L. Huang, S. Platnick, Y. Hu, and L. Strow (2004), Retrieval of semitransparent ice cloud optical thickness from Atmospheric Infrared Sounder (AIRS) measurements, *IEEE Trans. Geosci. Remote Sens.*, *42*, 2254–2267, doi:10.1109/TGRS.2004.833780.Weisz.
Weng, F. (2007), Advances in radiative transfer modeling in support of satellite data assimilation, *J. Atmos. Sci.*, *64*, 3799–3807.
Wu, W.–S., R. J. Purser, and D. F. Parrish (2002), Three-dimensional variational analysis with spatially inhomogeneous covariances, *Mon. Weather Rev.*, *115*, 209–232, doi:10.1175/1520-0493(2002)130<2905:TDVAWS>2.0.CO;2.
Wylie, D. P., W. P. Menzel, H. M. Woolf, and K. I. Strabala (1994), Four years of global cirrus cloud statistics using HIRS, *J. Clim.*, *7*(12), 1972–1986, doi:10.1175/15200442(1994)007<1972:FYOGCC>2.0.CO;2.
Zhang, M., M. Zupanski, M.-J. Kim, and J. A. Knaff (2013), Assimilating AMSU-A radiances in the TC core area with NOAA operational HWRF (2011) and a Hybrid Data Assimilation System: Danielle (2010), *Mon. Weather Rev.*, *141*(11), 3889–3907.